NGR 22-004-030

FULLY UNSTEADY SUBSONIC AND SUPERSONIC POTENTIAL AERODYNAMICS FOR COMPLEX AIRCRAFT CONFIGURATIONS FOR FLUTTER APPLICATIONS

by

Kadin Tseng

and

Luigi Morino

Presented at

AIAA/ASME/SAE 17th Structures,

Structural Dynamics and

Materials Conference

(NASA-CR-146573) FULLY UNSTEADY SUBSONIC AND SUPERSONIC POTENTIAL AERODYNAMICS FOR COMPLEX AIRCRAFT CONFIGURATIONS FOR FLUTTER APPLICATIONS (Boston Univ.) 14 p HC $3.50 CSCL 01A G3/02

N76-20077

Unclas
21489

FULLY UNSTEADY SUBSONIC AND SUPERSONIC POTENTIAL AERODYNAMICS OF COMPLEX AIRCRAFT CONFIGURATIONS FOR FLUTTER APPLICATIONS+

Kadin Tseng* and Luigi Morino**
Boston University
Boston, Massachusetts

Abstract

A general theory for steady, oscillatory or fully unsteady potential compressible aerodynamics around complex configurations is presented. Using the finite-element method to discretize the space problem, one obtains a set of differential-delay equations in time relating the potential to its normal derivative (on the surface of the body) which is expressed in terms of the generalized coordinates of the structure. For oscillatory flow, the motion consists of sinusoidal oscillations around a steady, subsonic or supersonic flow. For fully unsteady flow, the motion is assumed to consist of constant subsonic or supersonic speed for time $t \leq 0$ (steady state) and of small perturbations around the steady state for time $t>0$; the solution is obtained in Laplace's domain. From the potential, the aerodynamic generalized forces are obtained. Therefore the final output is the matrix of the aerodynamic coefficients, relating the generalized forces to the generalized coordinates, in the form necessary for flutter applications. The theory is embedded in a computer code, SOUSSA (Steady, Oscillatory and Unsteady, Subsonic and Supersonic Aerodynamics), which is briefly described. Numerical results are presented for steady and unsteady, subsonic and supersonic flows and indicate that the code is not only general, flexible, and simple to use but also accurate and fast.

1. Introduction

Presented herein is a general formulation of steady, oscillatory or fully unsteady, subsonic and supersonic potential aerodynamics for an aircraft having arbitrary shape. The objective of this formulation is to described the time functional relationship between aerodynamic potential and its normal derivative (normal wash) in a form which can be used for computational analysis. The finite-element method is used for space discretization. The matrix of the aerodynamic influence coefficients, as necessary for flutter calculations, is then obtained. Results obtained with the computer program SOUSSA (Steady, Oscillatory and Unsteady, Subsonic and Supersonic Aerodynamics) are also presented.

The analysis presented herein is based on a new integral formulation, presented in References 1 and 2, which includes completely arbitrary motion. However, the numerical implementation (Refs. 3 and 4) was thus far limited to steady and oscillatory flows. On the other hand, in order to perform a linear-system analysis of the aircraft, it is convenient to use more general aerodynamic formulations, i.e., fully transient response for time-domain analysis and the aerodynamic transfer function (Laplace transform of the fully unsteady operator) for frequency-domain analysis. A general formulation for fully unsteady (indicial) aerodynamics was presented in Refs. 5 and 6 where only very preliminary results were given. Consistent with this type of analysis, the unsteady contribution is assumed to start at time $t=0$, so that for time $t \leq 0$ the flow is in steady state. Furthermore, consistent with the linear flight dynamics analysis, the motion of the aircraft is assumed to consist of small (infinitesimal) perturbations around the steady-state motion.

It may be noted that within the assumption of potential aerodynamics, there exists other methods to evaluate the aerodynamic loads.[7] Among them, the lifting surface theories, while flexible and efficient, are not sufficiently general. On the other hand, finite-element methods, though sufficiently general for handling complex configurations, are limited to steady flows. In addition, they are usually quite cumbersome to use and invariably require human itervention to define the suitable type of element (source, doublet, etc.) to be used.[7] For oscillatory aerodynamics, the doublet-lattice method [8,9] is the only other method, besides SOUSSA, which can handle subsonic oscillatory flows around complex configur-

+This work was supported by NASA Langley Research Center under NASA Grant NGR 22-004-030. The authors wish to express their appreciation to Dr. E. Carson Yates, Jr., monitor of the program, for the invaluable suggestions and stimulating discussions made in connection with this work. The authors would also like to thank Messrs. Kian Lam Kho and Joseph A. Puglesi for their assistance in obtaining the numerical results.

* Graduate Student, Research Assistant
** Director, Computational Continuum Mechanics Program, Member AIAA

ations, while SOUSSA is the only program which can analyze oscillatory supersonic aerodynamics.

Finally, for fully unsteady aerodynamics, several problems have been considered since the initial work by Wagner (Ref. 10) on unsteady incompressible two-dimensional flow. While several methods are available for wings in subsonic and supersonic flow (see Refs. 11 and 12), no other code, besides SOUSSA, is available for subsonic and supersonic flows around arbitrary complex configurations for either time or frequency domain analysis.

The purpose of this paper, is to present recent developments on the formulation of Ref. 1. In this paper only the subsonic formulation is presented in details; the supersonic formulation is only briefly outlined in Appendix A. For conciseness, material previously presented (in particular, the material of Ref. 4) is not repeated herein.

Using the finite-element method to discretize the space problem, one obtains a set of differential-delay equations in time relating the potential to its normal derivative (on the surface of the body), which is expressed in terms of the generalized coordinates of the structure. For oscillatory flow, the motion consists of sinusoidal oscillations around a steady, subsonic or supersonic flow. For fully unsteady flow, the motion is assumed to consist of constant subsonic or supersonic speed for time $t \leq 0$ (steady state) and of small perturbations around the steady state for time $t > 0$; the solution is obtained in Laplace's domain. From the potential, the aerodynamic generalized forces are obtained. Therefore the final output is the matrix of the aerodynamic coefficients, relating the generalized forces to the generalized coordinates. The theory is embedded in a computer code, SOUSSA (Steady Oscillatory and Unsteady, Subsonic and Supersonic Aerodynamics), which is briefly described. Numerical results are presented for steady and unsteady, subsonic and supersonic flows and indicate that the code is not only general, flexible, and simple to use but also accurate and fast.

2. Equation for Velocity Potential

The subsonic aerodynamic formulation used in SOUSSA is briefly presented here. The supersonic formulation is given in Appendix A. Assume the flow to be an infinitesimal perturbation from the steady state flow. Then standard use of Green's function method applied to the equation of the velocity potential yields, after linearization, the following integral equation [1,2].

$$2\pi\,\Phi(\bar{P}_*,T) = -\oiint_{\Sigma_B} [\Psi]^{\Theta}\,\frac{1}{R}\,d\Sigma_B + \oiint_{\Sigma_B}\left\{[\Phi]^{\Theta}\,\frac{\partial}{\partial N}\left(\frac{1}{R}\right) - \left[\frac{\partial\Phi}{\partial T}\right]^{\Theta}\frac{1}{R}\,\frac{\partial R}{\partial N}\right\}d\Sigma_B + \iint_{\Sigma_W}\left\{[\Delta\Phi]^{\Theta}\,\frac{\partial}{\partial N}\left(\frac{1}{R}\right) - \left[\frac{\partial\Delta\Phi}{\partial T}\right]^{\Theta}\frac{1}{R}\,\frac{\partial R}{\partial N}\right\}d\Sigma_W \tag{1}$$

where $\bar{P}_*$ is on the surface of the body, Σ_B, $\bar{N}$ is the outer normal

$$\Phi = \varphi/U_\infty \ell \qquad \Psi = \partial\Phi/\partial N \tag{2}$$

$$X = x/\beta\ell \quad Y = y/\ell \quad Z = z/\ell \quad T = U_\infty \beta t/\ell$$

with $\beta = \sqrt{1 - M^2}$ and

$$R = \left[(X - X_*)^2 + (Y - Y_*)^2 + (Z - Z_*)^2\right]^{1/2} \tag{3}$$

while

$$[\;]^{\Theta} = [\;]\Big|_{T-\Theta} \tag{4}$$

where

$$\Theta = M\,(X - X_*) + R \tag{5}$$

is the time necessary for a disturbance to propagate from $\bar{P}$ to $\bar{P}_*$. In addition, Σ_W is the (open) surface of the wake (known from the steady state solution) and $\Delta\Phi$ is the potential-discontinuity across the wake, evaluated in the direction of the normal, i.e. $\Delta\Phi \equiv \Phi_u - \Phi_\ell$ if the upper normal is used. It should be noted that the value of $\Delta\Phi$ is not an additional unknown, since

$$\Delta\Phi\,(\bar{P}, T) = \Delta\Phi\,(\bar{P}_{TE}, T - \Pi) \tag{6}$$

where Π is the nondimensional time necessary for the vortex-point to travel (within the steady flow) from the point, $\bar{P}_{TE}$ (origin of the vortex-line at the trailing edge), to the point $\bar{P}$. For small-perturbation steady flow, Π is given by [6]

$$\Pi = \beta^2 (X - X_{TE})/M \tag{7}$$

Equations (1) and (6) fully describe the problem of linearized unsteady subsonic potential aerodynamics around complex configurations. In order to solve this problem, it is necessary, in general, to obtain a numerical approximation for Eq. (1). This is obtained by dividing the surface of the aircraft into N_B quadrilateral elements Σ_h (which are described in terms of the corner points by use of standard finite-element interpolation technique*) and by assuming ψ and Φ to be constant within each element:

$$\Psi(\bar{P}, T-\Theta) = \Psi_h(T-\Theta_h)$$
$$\Phi(\bar{P}, T-\Theta) = \Phi_h(T-\Theta_h) \tag{8}$$

where $\psi_h(T-\Theta_h)$ and $\Phi_h(T-\Theta_h)$ are time dependent values of ψ and Φ at the centroid $\bar{P}_h$ of Σ_h at the time $T-\Theta_h$ (where Θ_h is the disturbance-propagation time from $\bar{P}_*$ to $\bar{P}_h$).

Next consider the integrals on the wake. In order to facilitate the use of Eq. (6), it is convenient to divide the wake into strips defined by (steady-state) vortex-lines emanating from the nodes on the trailing edge. The strips are then divided into N_W elements $\Sigma_n(w)$ with nodes along the vortex lines. The potential discontinuity is assumed to be constant within each element

$$\Delta\Phi(\bar{P}, T-\Theta) = \Delta\Phi_n(T-\Theta_n) \tag{9}$$

where $\Delta\Phi_n(T-\Theta_n)$ is the value of $\Delta\Phi$ at the centroid $\bar{P}_n^{(W)}$ of the element $\Sigma_n^{(W)}$ on the wake at time $T-\Theta_n$ (where Θ_n is the propagation time from $\bar{P}_n^{(W)}$ to $\bar{P}_*$). Note that according to Eq. (6)

$$\Delta\Phi_n(T) = \Delta\Phi_{m(n)}^{(TE)}(T-\Pi_n) \tag{10}$$

where m=m(n) identifies the trailing-edge point which is on the same vortex-line as the point $\bar{P}_n^{(W)}$. Furthermore, Π_n is the time necessary for the vortex-point to be convected from the trailing-edge point $\bar{P}_m^{(TE)}$ to the wake-point $\bar{P}_n^{(W)}$.

It may be worth noting that $\Delta\Phi_m^{(TE)} = \Phi_{h_u} - \Phi_{h_\ell}$, where h_u and h_ℓ identify the upper and lower trailing-edge nodes on the body corresponding to the mth node on the trailing-edge.

In SOUSSA $\Phi_{h_u} - \Phi_{h_\ell}$ is approximated with the value evaluated at the centroids of the elements adjacent to the trailing edge. This is reasonable in view of the Kutta condition.[6] Π_n is then evaluated from the centroid, as[6]

$$\Pi_n = \beta^2 (X_n^{(W)} - X_h)/M \tag{11}$$

With the above approximation, it is possible to write[6]

$$\Delta\Phi_{m(n)}^{(TE)} = \sum_h S_{nh}\Phi_h \tag{12}$$

where $S_{nh} = 1$ ($S_{nh}=-1$), if h identifies the upper (lower) point $\bar{P}_h$ on the body corresponding to the point $\bar{P}_n^{(W)}$ on the wake (i.e., near the point $\bar{P}_{m(n)}^{(TE)}$ on the trailing edge), and $S_{nh}=0$ otherwise.

Combining Eqs. (1), (8) and (9) and assuming $\bar{P}_* \equiv \bar{P}_j$, one obtains

$$\begin{aligned}\Phi_j(T) = &\sum_h B_{jh}\Psi_h(T-\Theta_{jh}) \\ &+ \sum_h C_{jh}\Phi_h(T-\Theta_{jh}) + \sum_h D_{jh}\dot{\Phi}_h(T-\Theta_{jh}) \\ &+ \sum_n\sum_h F_{jn}S_{nh}\Phi_h(T-\Theta_{jn}-\Pi_n) \\ &+ \sum_n\sum_h G_{jn}S_{nh}\dot{\Phi}_h(T-\Theta_{jn}-\Pi_n)\end{aligned} \tag{13}$$

where

$$B_{jh} = -\frac{1}{2\pi}\iint_{\Sigma_h}\frac{1}{R}\,d\Sigma_h\Big|_{P_*=P_j} \tag{14}$$

$$C_{jh} = \frac{1}{2\pi}\iint_{\Sigma_h}\frac{\partial}{\partial N}\left(\frac{1}{R}\right)d\Sigma_h\Big|_{P_*=P_j}$$

$$D_{jh} = -\frac{1}{2\pi}\iint_{\Sigma_h}\frac{1}{R}\frac{\partial R}{\partial N}\,d\Sigma_h\Big|_{P_*=P_j}$$

$$F_{jn} = \frac{1}{2\pi}\iint_{\Sigma_n}\frac{\partial}{\partial N}\left(\frac{1}{R}\right)d\Sigma_n\Big|_{P_*=P_j}$$

$$G_{jn} = -\frac{1}{2\pi}\iint_{\Sigma_n}\frac{1}{R}\frac{\partial R}{\partial N}\,d\Sigma_n\Big|_{P_*=P_j}$$

and

$$\Theta_{jh} = \Theta_h\Big|_{\bar{P}_*=\bar{P}_j} \tag{15}$$

Using the above mentioned hyperboloidal quadrilateral elements the coefficients B_{jh}, C_{jh}, F_{jn} and G_{jn} are evaluated analytically with the expressions given

* The equation for the elements are of the type $\bar{P} = \bar{P}_0 + \xi\bar{P}_1 + \eta\bar{P}_2 + \xi\eta\bar{P}_3$ ($-1<\xi<1$; $-1<\eta<1$). This type of element is called hyperboloidal element and is described in details in Ref. 4.

in Ref. 4. The coefficients D_{jh} are approximated as $D_{jh}=R_{jh}C_{jh}$ where $R_{jh}=|\bar{P}_j-\bar{P}_h|$.

Next, taking the Laplace transform with zero initial conditions of Eq. (13) yields[6]

$$\left[\tilde{Y}_{jh}\right]\left\{\tilde{\Phi}_h\right\}=\left[\tilde{Z}_{jh}\right]\left\{\tilde{\Psi}_h\right\} \tag{16}$$

where $\tilde{\Phi}_h$ and $\tilde{\Psi}_h$ are the Laplace transforms of Φ_h and Ψ_h while

$$\tilde{Y}_{jh}=\delta_{jh}-\left(C_{jh}+S\,D_{jh}\right)e^{-S\Theta_{jh}} - \sum_n\left(F_{jn}+S\,G_{jn}\right)e^{-S(\Theta_{jn}+\Pi_n)}S_{nh} \tag{17}$$

and

$$\tilde{Z}_{jh}=B_{jh}\,e^{-S\Theta_{jh}} \tag{18}$$

whereas S is the nondimensional Laplace parameter.*

3. Boundary Condition

The derivation of the boundary condition is given in details in Ref. 13. Here the derivation is briefly summarized. The boundary condition obtained by imposing that the velocity of the fluid and the velocity of the body, $\bar{v}$, have the same components along the normal to the surface of the body. This yields

$$\Psi=(\bar{v}-U_\infty\bar{i})\cdot\bar{n}(t)/U_\infty \tag{19}$$

where $\bar{n}(t)$ is the instantaneous normal to the surface of the body. The unsteady part of the boundary conditions (neglecting high order terms) is given by

$$\Psi=\frac{1}{U_\infty}\bar{v}\cdot\bar{n}+\Delta\bar{n}\cdot\bar{i} \tag{20}$$

with $\Delta\bar{n}\cdot\bar{i}=\dfrac{1}{|\bar{a}_1\times\bar{a}_2|}\left(\dfrac{\partial\bar{d}}{\partial\xi^1}\cdot\bar{a}_2\times\bar{i}-\dfrac{\partial\bar{d}}{\partial\xi^2}\cdot\bar{a}_1\times\bar{i}\right)$

where $\bar{d}$ is the displacement of a point of the body. Expressing $\bar{d}$ and $\bar{v}$ in terms of the generalized coordinates of q_n as

$$\bar{d}=\sum_{n=1}^{N_o}q_n\,\bar{M}_n(\xi^\alpha) \tag{21}$$

* For oscillatory aerodynamics, setting $\phi_h(T)=\tilde{\phi}_h e^{i\Omega T}$ and $\Psi_h(T)=\tilde{\Psi}_h e^{i\Omega T}$ yields the same equation with $S=i\Omega$

and

$$\bar{v}=\sum_{n=1}^{N_o}\dot{q}_n\,\bar{M}_n(\xi^\alpha) \tag{22}$$

one obtains, in the Laplace domain,

$$\tilde{\Psi}=\sum_{n=1}^{N_o}\left[\frac{s}{U_\infty}\bar{M}_n\cdot\bar{n} + \frac{1}{|\bar{a}_1\times\bar{a}_2|}\left(\frac{\partial\bar{M}_n}{\partial\xi^1}\cdot\bar{a}_2\times\bar{i}-\frac{\partial\bar{M}_n}{\partial\xi^2}\cdot\bar{a}_1\times\bar{i}\right)\right]\tilde{q}_n \tag{23}$$

where $s=S\beta a_\infty/\ell$. Equation (23) gives the desired relationship between normal wash at any point and the generalized coordinates q_n.

4. Pressure and Generalized Forces

In order to complete the formulation, the procedure for the evaluation of the aerodynamic pressure and the generalized forces is presented in this section.

First, consider an averaging scheme which imposes that the value of the potential Φ_k' at the node $\bar{P}_k'$ is the average of the values of the potential at the centroids of the elements surrounding $\bar{P}_k'$. In other words

$$\{\Phi_k'\}=[E_{kh}]\{\Phi_h\} \tag{24}$$

where $[E_{kh}]$ is an averaging matrix defined as

$$E_{kh}=\frac{1}{N^{(k)}}\quad \text{if}\quad \bar{P}_k'\in\Sigma_h \tag{25}$$

(i.e., if the $\bar{P}_k'$ is one of the corner points of the element Σ_h) and

$$E_{kh}=0\quad\text{otherwise} \tag{26}$$

In Eq. (25), $N^{(k)}$ is the number of elements which have $\bar{P}_k'$ as one of their corner points. Having evaluated the values of Φ at the four corner points of each quadrilateral element, the potential is expressed as

$$\Phi=\Sigma\,\Phi_h'\,N_h'(\bar{P}) \tag{27}$$

where N'_h are the first-order global shape-functions obtained by assembling local shape-functions of the type

$$N_k^{(E)} = \frac{1}{4\xi_k \eta_k} (\xi + \xi_k)(\eta + \eta_k) \tag{28}$$

where $\xi_k = \pm 1$ and $\eta_k = \pm 1$ are the locations of the corners $\bar{P}_k$ of the element Σ_h (ξ and η are the coordinates over the element) so that

$$\frac{\partial \Phi}{\partial \Xi^\alpha} = \sum \Phi'_h \frac{\partial N'_h}{\partial \Xi^\alpha} \tag{29}$$

where $\Xi^1 = \xi;\ \Xi^2 = \eta$.

The pressure coefficient may be evaluated from the linearized Bernoulli theorem as

$$c_p = -2\left(\frac{\beta}{M}\frac{\partial \Phi}{\partial T} + \frac{1}{\beta}\ \overline{\nabla}\Phi \cdot \overline{i}\ \right) \tag{30}$$

Expressing $\overline{\nabla}\Phi$ in terms of the tangential derivatives of Φ and neglecting the contribution of the normal component, the pressure coefficient is given by

$$c_p = -\frac{2}{\beta}\left(\frac{\beta^2}{M}\frac{\partial \Phi}{\partial T} + \overline{i} \cdot \overline{A}^1 \frac{\partial \Phi}{\partial \Xi^1} + \overline{i} \cdot \overline{A}^2 \frac{\partial \Phi}{\partial \Xi^2}\right) \tag{31}$$

where $\overline{A}^\alpha$ are the contravaniant base vectors, with $\partial\Phi/\partial\Xi^\alpha$ given by Eq.(29).

Next consider the generalized aerodynamic forces

$$Q_n = -\oint\!\!\oint q\, c_p\, \overline{n} \cdot \overline{M}_n\, d\Sigma_B \tag{32}$$

where

$$q = \frac{1}{2} \rho U_\infty^2 \tag{33}$$

is the dynamic pressure.

By assuming that the pressure coefficient c_p is constant within each element (consistent with the assumption made on Φ), Eq. (32) can be expressed as

$$\{Q_n\} = q[Q_{nh}]\{(c_p)_h\} \tag{34}$$

where

$$\begin{aligned} Q_{nh} &= -\iint_{\Sigma_h} \overline{n} \cdot \overline{M}_n\, d\Sigma_h \\ &= -\int_{-1}^{1}\!\!\int_{-1}^{1} \overline{a}_1 \times \overline{a}_2 \cdot \overline{M}_n\, d\xi^1 d\xi^2 \\ &\approx -4(\overline{a}_1 \times \overline{a}_2 \cdot \overline{M}_n)\Big|_{\vec{P} = \vec{P}_h} \end{aligned} \tag{35}$$

where $\overline{a}_1$, and $\overline{a}_2$ are the base vectors of the element Σ_h.

5. SOUSSA

The above formulation is implemented in the computer program SOUSSA (Steady, Oscillatory and Unsteady, Subsonic and Supersonic Aerodynamics). The program is an improvement of the program SOSSA presented in Ref. 4 and therefore retains all of the basic features analyzed in Ref. 4. In particular the program besides being general and flexible is also very simple to use. The only inputs are the location of the corner points of the quadrilateral elements, the Mach number and the reduced frequency. The wake is automatically generated. It should be noted that a considerable improvement with respect to SOSSA is that supersonic flows are treated exactly the same way as the subsonic ones: in particular diaphragms are not used in SOUSSA.* Therefore the basic simplicity in use for the subsonic flows is retained in supersonic flows as well. An additional feature which didn't exist in SOSSA is the evaluation of the aerodynamic influence coefficients. Therefore it may be worth it to add a few comments on the computational implementation of the formulation presented above. (Details for the following expressions are given in Ref. 13.) Note first that the relationship between normal wash and generalized coordinates, Eq. (23) may be written as*

$$\underset{\sim}{\tilde{\Psi}} = \underset{\sim}{\tilde{M}}^{(1)} \underset{\sim}{\tilde{q}} \tag{36}$$

where

$$\underset{\sim}{\tilde{\Psi}} = \{\tilde{\Psi}_n\} \tag{37}$$

* In Eqs. (36) to (43) compact matrix notations are used. Vectors and matrices are underlined. Tildas indicate Laplace's transform or equivalent operation.

$$\tilde{q} = \left\{\tilde{q}_n\right\} \tag{38}$$

and $\tilde{M}^{(1)}$ a matrix implicitly defined by Eq. (23). Furthermore Eq. (16) may be rewritten as

$$\tilde{\Phi} = \tilde{Y}^{-1} \tilde{Z} \tilde{\Psi} = \tilde{M}^{(2)} \tilde{\Psi} \tag{39}$$

whereas the relationship between pressure coefficient and potential may be written as

$$\tilde{c}_p = \tilde{M}^{(3)} \tilde{\Phi} \tag{40}$$

where $\tilde{M}^{(3)}$ is obtained by combining Eqs. (24), (27), (29) and (31). Finally (see Eq. (34))

$$\tilde{Q} = q \tilde{M}^{(4)} \tilde{c}_p \tag{41}$$

or, combining Eqs. (36), (39), (40) and (41),

$$\tilde{Q} = q \tilde{M} \tilde{q} \tag{42}$$

where the matrix of the aerodynamic influence coefficients $\tilde{M}$ is given by

$$\tilde{M} = \tilde{M}^{(4)} \tilde{M}^{(3)} \tilde{M}^{(2)} \tilde{M}^{(1)} \tag{43}$$

Note that $\tilde{M}^{(1)}$ and $\tilde{M}^{(4)}$ depend upon the modes $\tilde{M}_n(\xi^\alpha)$, whereas $\tilde{M}^{(2)}$ and $\tilde{M}^{(3)}$ do not. The separation of $\tilde{M}$ into mode-dependent matrices and mode-independent matrices is particularly useful for automated structural design in which the same geometry but different modes are used in each iteration. In addition $\tilde{M}^{(2)}$ is the only matrix which depends in a complicated way upon the complex frequency S. However once the coefficients of Eqs. (14) and (15) are evaluated, the evaluation of $\tilde{M}^{(2)}$ requires only the combination of this coefficients according to Eqs. (17) and (18) and the inversion of the matrix $\tilde{Y}$ (see eq. 39). This is particularly useful for the evaluation of the aerodynamic influence coefficients for various frequencies, as needed for instance for flutter analysis. An example of the time saving obtained by using the two above features is given in the following section.

6. Numerical Results

Typical numerical results obtained with SOUSSA (Ref. 14) are presented in this section. Figure 1 shows the sectional lift coefficients at various stations of a wing-body in steady subsonic flow compared against experimental and theoretical results of Ref. 6 and 15. The results were obtained for M=0 and a rectangular wing with chord c=1, and span b=6 thickness τ=0.09 and α_w=6°. The body is at zero angle of attack with overall length of 5 chords (forebody with length L_a=2c, fuselage length L_f=3). Note that the fuselage is closed at the end by a circular plate. In addition, a flat wake is emanating from the wing trailing edge and a cylindrical wake from that of the fuselage. Figure 2 shows the convergence analysis of sectional lift of Figure 1 as a function of the number of elements. The computer time used for each case is also indicated. Figures 3 and 4 present the lift and moment coefficients of a rectangular wing in supersonic unsteady flows with aspect ratio AR=2, c=1, b=2, τ=0.001 and complex reduced frequencies k_c=-0.2+i1.0, 0.0+i1.0 and +0.2+i1.0 for Mach number M=$2^{1/2}$ to 2.5. The results are compared with those of Ref. 16. Noted that in contrast to Ref. 6, the present method does not require the use of diaphragms. Figure 5 presents a wing-body-tail configuration in fully unsteady flow with specifications of the geometry similar to that of Fig. 1. However, a horizontal tail is added with chord c=1 and b=6 which is stationed 0.5 chords above the center line of the fuselage. The complex reduced frequency was k_c=0.1+i0.5. No existing result is available for comparison, for, as mentioned above, the present method is the only existing one which can analyze fully unsteady flow. The result is presented to demonstrate the generality of the method and its ability to handle fully unsteady flow problems. Figures 6 and 7 presents the lift and moment coefficients and their corresponding phase angles for a rectangular wing oscillating in plunge and pitch in subsonic flow with AR=2, τ=0.001, Mach number M=0. and 4x7x7 elements on the whole wing. The results are identical with the ones obtained with SOSSA. However, considerable time saving was obtained in the respective frequency and mode calculations by the decomposition of the matrix $\tilde{M}$ into frequency and mode dependent matrices $\tilde{M}_I$ (see Eq. (43)). All the results were obtained in 44 mins. i.e. 82.5 secs. for one aerodynamic coefficient and one frequency (since four coefficients and eight frequencies have been considered). Note that the time for one single coefficient and one single frequency (if evaluated independently) is about 13 minutes.

Tables 1 and 2 contains the generalized forces for an AGARD wing-tail configuration in quasi-steady and oscillatory flow compared with several existing methods (Refs. 17 to 21). While Table 3 included the generalized forces for the same configuration in fully unsteady flow (complex frequency). For all the results the standard AGARD geometry (described for instance in Refs. 18 and 19) was used. This consists of two swept tapered lifting surfaces. The first surface has $x_{LE}=0$ and $x_{TE}=2.25$ at $y=0$ and $x_{LE}=2.75$ and $x_{TE}=3.70$ at $y=1$ and is located at $z=0$. The second surface has $x_{LE}=2.70$ and $x_{TE}=4.00$ at $y=0$ and $x_{LE}=3.90$ and $x_{TE}=4.25$ at $y=1$ and is located at $z=.6$. All the results prescribed here were obtained using 4x7x7 elements on each surface. Results obtained with 4x5x5 elements indicate that convergence was attained. The results are usually in excellent agreement with those of Refs. 17 to 21.

7. Conclusions

A general formulation and computer program for the analysis of steady, oscillatory and unsteady, subsonic and supersonic aerodynamic flows around complex configurations have been presented. The final output of the code is the matrix of the aerodynamic influence coefficients for flutter analysis to be used for instance in the program FCAP (Ref. 22).

It should be noted that, while there exists several methods to analyze the problem of unsteady compressible flows for complex configurations, the present method, embedded in the computer program SOUSSA, is unique in the following aspects:

1. It provides a completely unified approach for steady, oscillatory and fully unsteady, subsonic and supersonic aerodynamic flows.
2. It can be applied to arbitrarily-complex configurations. Wing-body-tail configurations in fully unsteady flows have been presented.
3. It is computationally extremely general, flexible, efficient and above all, accurate. The elimination of diaphragms in supersonic flow improved considerably the simplicity and efficiency of the code.
4. SOUSSA is the only existing program that can analyze fully unsteady complex-configuration potential aerodynamics in subsonic or supersonic regimes. It is also the only program capable of handling oscillatory supersonic aerodynamics for complex configurations.
5. In contrast to existing methods, which in many instances requires extensive user's background in aerodynamics and familiarity with the specific method, the present code requires very limited human intervention and is extremely easy to use.
6. Flutter and optimal design analyses require evaluation of the aerodynamic influence coefficients for several frequencies and mode shapes. With the unique features mentioned above, (i.e., separation of the aerodynamic influence coefficient matrices into frequency and mode dependent and independent matrices) the computer time that normally would have been required is dramatically reduced.

Appendix A

In this Appendix the formulation for the supersonic case is briefly outlined. For conciseness, only supersonic trailing edges are considered so that the contribution of the wake can be ignored. (In SOUSSA diaphagms are not used and therefore the supersonic wake is treated as the subsonic one.) Under small-perturbation assumption, the Green theorem for potential supersonic flow is given by

$$2\pi\,\Phi(\tilde{P}_*,T) = -\oiint_{\Sigma_B}\left([\psi']^{\Theta+} + [\psi']^{\Theta-}\right)\frac{H}{R'}d\Sigma + \oiint_{\Sigma_B}\left([\Phi]^{\Theta+} + [\Phi]^{\Theta-}\right)\frac{\partial}{\partial N^c}\left(\frac{H}{R'}\right)d\Sigma - \oiint_{\Sigma_B}\left(\left[\frac{\partial\Phi}{\partial T}\right]^{\Theta+} - \left[\frac{\partial\Phi}{\partial T}\right]^{\Theta-}\right)\frac{H}{R'}\frac{\partial R'}{\partial N^c}d\Sigma \qquad (A.1)$$

where $\psi' = \dfrac{\partial\Phi}{\partial N^c}$ ($\dfrac{\partial}{\partial N^c}$ is the conormal derivative (Ref. 4)) is the conormal wash which is prescribed by the boundary conditions, and

$$X = x/\beta' \ell \quad Y = y/\ell \quad Z = z/\ell \quad T = a_\infty \beta' t/\ell \qquad (A.2)$$

with $\beta' = \sqrt{M^2-1}$. Furthermore,

$$R = \left[(X-X_*)^2 - (Y-Y_*)^2 - (Z-Z_*)^2\right]^{1/2} \qquad (A.3)$$

whereas

$$H = 1 \text{ for } X_* - X > \left[(Y-Y_*)^2 + (Z-Z_*)^2\right]^{1/2}$$
$$= 0 \text{ for } X_* - X \le \left[(Y-Y_*)^2 + (Z-Z_*)^2\right]^{1/2} \qquad (A.4)$$

and

$$[\,]^{\Theta\pm} = [\,]\Big|_{T-\Theta^\pm} \qquad (A.5)$$

with

$$\Theta^\pm = M(X_* - X) \pm R' \qquad (A.6)$$

Following the same procedure used for the subsonic case one obtains

ORIGINAL PAGE IS
OF POOR QUALITY

$$\Phi_j(T) = \sum_h B'_{jh}\left[\Psi'_h(T-\Theta^+_{jh})+\Psi'_h(T-\Theta^-_{jh})\right] + \sum_h C'_{jh}\left[\Phi_h(T-\Theta^+_{jh})+\Phi_h(T-\Theta^-_{jh})\right] + \sum_h D'_{jh}\left[\dot{\Phi}_h(T-\Theta^+_{jh})-\dot{\Phi}_h(T-\Theta^-_{jh})\right] \quad (A.7)$$

where

$$B'_{jh} = -\frac{1}{2\pi}\iint_{\Sigma_h}\frac{H}{R'}\,d\Sigma_h\Big|_{P_*=\bar{P}_j}$$
$$C'_{jh} = -\frac{1}{2\pi}\iint_{\Sigma_h}\frac{\partial}{\partial N^c}\left(\frac{H}{R'}\right)d\Sigma_h\Big|_{P_*=P_j} \quad (A.8)$$
$$D'_{jh} = -\frac{1}{2\pi}\iint_{\Sigma_h}\frac{H}{R'}\frac{\partial R'}{\partial N^c}\,d\Sigma_h\Big|_{P_*=P_j}$$

The definition of Θ^+_{jh} and Θ^-_{jh} is discussed at the end of this appendix.

Finally, taking the Laplace transform of equation (26) results in

$$\left[\tilde{Y}'_{jh}\right]\left\{\tilde{\Phi}_h\right\} = \left[\tilde{Z}'_{jh}\right]\left\{\tilde{\Psi}_h\right\}. \quad (A.9)$$

where

$$\left[\tilde{Y}'_{jh}\right] = \left[\delta_{jh} - C'_{jh}\left(e^{-s\Theta^+_{jh}}+e^{-s\Theta^-_{jh}}\right) - sD'_{jh}\left(e^{-s\Theta^+_{jh}}-e^{-s\Theta^-_{jh}}\right)\right] \quad (A.10)$$

$$\left[\tilde{Z}'_{jh}\right] = \left[B'_{jh}\left(e^{-s\Theta^+_{jh}}+e^{-s\Theta^-_{jh}}\right)\right] \quad (A.11)$$

Equation (A.9) yields the matrix $\tilde{\underline{M}}^{(2)}$ to be used in Eq. (39) for supersonic flows. The supersonic matrices $\tilde{\underline{M}}^{(1)}$, $\tilde{\underline{M}}^{(3)}$ and $\tilde{\underline{M}}^{(4)}$ are equal to the subsonic ones. Therefore the above modifications in the definitions of $\tilde{Y}'_{jh}$ and $\tilde{Z}'_{jh}$ are the only changes necessary for supersonic flows. As mentioned above if the trailing edges are partially subsonic the wake is treated as in the subsonic case.

Finally a few remarks are necessary on the fact that diaphragms are not used in SOUSSA and on how this relates to the correct definition of Θ^+_{jh} and Θ^-_{jh}. It should be noted that Θ^+_{jh} and Θ^-_{jh} are imaginary if the centroid $\bar{P}_h$ of the element Σ_h lies outside the Mach forecone of the control point $\bar{P}_j$. This yields no problem for the elements completely outside or completely inside the Mach forecone. However for the elements partially inside the Mach forecone, a special definition for Θ^+_{jh} and Θ^-_{jh} must be used: note that Θ^+_{jh} and Θ^-_{jh} represent the two propagation times for the disturbances emanating from the element Σ_h to reach the point $\bar{P}_j$. Therefore for elements partially inside the Mach forecone, Θ^+_{jh}, and Θ^-_{jh} are most appropriately defined (from a physical point of view) as the propagation times from the centroid of the portion of the element Σ_h intersected by the Mach forecone, to the control point $\bar{P}_j$.

It should be noted that with this definition of Θ^+_{jh} and Θ^-_{jh}, supersonic flows can be treated exactly the same way as subsonic flows. For instance a wing with supersonic leading edge is solved by using both sides of the wing simultaneously. Also for wings with partially supersonic leading edges the use of diaphragms is not necessary. This is a considerable advantage: the use use of diaphragms in the program SOSSA was cumbersome, especially for wing-body-tail and non-coplanar surfaces analyses. In the program SOUSSA there is no difference in the treatment of subsonic and supersonic flows.

References

1. Morino, L., "A General Theory of Unsteady Compressible Potential Aerodynamics," NASA CR-2464, 1974.

2. Morino, L., "Unsteady Compressible Potential Flow Around Lifting Bodies: General Theory," AIAA Paper No. 73-196, 1973.

3. Morino, L., and Kuo, C.C., "Subsonic Potential Aerodynamics for Complex Configurations: A General Theory," AIAA J., Vol. 12, No. 2, Feb. 1974, pp. 191-197.

4. Morino, L., Chen, L.T., and Suciu, E.O., "Steady and Oscillatory Subsonic and Supersonic Aerodynamics Around Complex Configurations," AIAA J., Vol. 13, No. 3, March 1975, pp. 368-374.

5. Morino, L., "Subsonic and Supersonic Indicial Aerodynamics and Aerodynamic Transfer Function for Complex Configurations," Boston University, ENG-TN-74-01, September 1974.

6. Morino, L., and Chen, L.T., "Indicial Compressible Potential Aerodynamics Around Complex Aircraft Configuration," in Aerodynamic Analyses

Requiring Advanced Computers, NASA SP-347, Paper No. 38, 1975, pp. 1067-1110.

7. Ashley, H. and Rodden, W.P., "Wing-Body Aerodynamic Interaction," Annual Review of Fluid Mechanics, Vol. 4, 1972, pp. 431-472.

8. Albano, E., and Rodden, W.P., "A Doublet-Lattice Method for Calculating Lift Distribution on Oscillating Surfaces in Subsonic Flows," AIAA J., Vol. 7, No. 2, Feb. 1969, pp. 279-285.

9. Giesing, J.P., Kalman, T.P., and Rodden, W.P., "Subsonic Steady and Oscillatory Aerodynamics for Multiple Interfering Wings and Bodies", Journal of Aircraft, Vol. 9, No. 10, Oct. 1972, pp. 693-702.

10. Wagner, H., "Uber die Entschung des dynamischen Auftribes von Tragflugeln," Z. Angew. Math. & Mech., Bd. 5, Heft 1, Feb. 1925, p. 17.

11. Lomax, H., "Indicial Aerodynamics," Aerodynamic Aspects, AGARD Manual on Aeroelasticity, Pt. II, Ch. 6, W.P. Jones, ed., North Atlantic Treaty Organization (Paris).

12. Garrick, I.E., "Nonsteady Wing Characteristics," Section F of Aerodynamic Components of Aircraft at High Speeds. Vol. VII of High Speed Aerodynamics and Jet Propulsion, eds. A.F. Donovan and H.R. Lawrence, Princeton Univ. Press, 1957.

13. Noll, R.B., and Morino, L., "Flight Control Analysis Program (FCAP) for Arbitrary Configuration Flexible Aircraft With Active Control," Vol. I, Theoretical Analysis, Aerospace Systems, Inc., Burlington, Mass., ASI-TR-75-23, 1975.

14. Tseng, K.D. and Morino, L., "SOUSSA : Steady, Oscillatory and Unsteady, Subsonic and Supersonic Aerodynamics: A User's Manual" , in preparation.

15. Labrujere, T.E., Loeve, W. and Sloff, J.W., "An approximate Method for the Calculation of the Pressure Distribution on Wing-body Combinations at Subcritical Speeds", AGARD Specialist Meeting on Aerodynamic Interference, Silver Springs, Md., Sept. 1970, AGARD Conf. Proc. No. 71.

16. Laschka, B., "Zur Theorie der Harmonisch Schwingenden Tragenden Flache bei Unterschallenstromung", Zeitschrift fur Flugwissenchaften, 11 (1963), Heft 7, pp. 265-292.

17. Huttsell, L.J. and Pollock, S.J., "Unsteady Aerodynamic Loads for the AGARD Interfering Lifting Surfaces". AFFDL paper, 1974.

18. Rodden, W.P., Giesing, J.P. and Kalman, T.P., "New Developments and Applications of the Subsonic Doublet-Lattice Method for Nonplanar Configurations" Paper No. 4, AGARD Symposium on Unsteady Aerodynamics for Aeroelastic Analyses of the Interfering Surfaces, AGARD-CP-80-71, 1970.

19. Davies, D.E., "Applications of Unsteady Airforce Calculation Methods to AGARD Interfering Surfaces", Paper No. 8, AGARD Symposium on Unsteady Aerodynamics for Aeroelastic Analyses of Interfering Surfaces, AGARD-CP-80-71, 1970.

20. Pollock, S.J. and Huttsell, L.J. "Applications of Three Unsteady Aerodynamic Load Prediction Methods" AFFDL TR-73-147, May 1974.

21. Appa, K. and Jones, W.P., "Integrated Potential Formulation of Unsteady Aerodynamics for Interacting Wings," AIAA Paper No. 75-762.

22. Morino, L., and Noll, R.B., "Flutter and Gust Response Analysis of Flexible Aircraft With Active Control", to be presented at the AIAA/ASME/SAE 17th Structures, Structural Dynamics and Materials Conference, King of Prussia, Pa., May 4-7 1976.

NOMENCLATURE

a_∞	speed of sound in undisturbed flow
k	reduced frequency, $\omega \ell/U_\infty$
k_c	complex reduced frequency
ℓ	reference length
M	Mach number, U_∞/a_∞
$\tilde{N}$	normal to Σ_B
N_W	number of wake elements in x-direction
N_x	number of elements in x-direction on half wing
N_y	number of elements in y-direction on half wing
$\bar{P}$	point having coordinates (X,Y,Z)
P_*	control point, (X_*,Y_*,Z_*)
R	defined by Eq. (3)
S	nondimensional complex frequency (for Laplace Transform)
T	nondimensional time, Eq. (2)
U_∞	velocity of undisturbed flow
X,Y,Z	nondimensional space coordinates, Eq. (2)
$\Delta\phi$	discontinuity of ϕ across the wake
θ	time for a disturbance to propagate from $\bar{P}$ to P_*, Eq. (5)
Π	convection time of wake vortices, Eq. (7)
Σ_B	surface of body
Σ_W	surface of wake
ϕ	nondimensional velocity perturbation potential
Ψ	nondimensional normal wash
$\tilde{(\ )}$	Laplace Transform of ( )

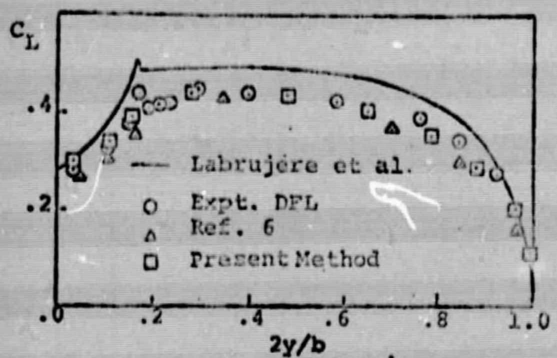

Fig. 1. Sectional lift coefficient distributions for a wing-body configuration with $\alpha_W=5$, $\alpha_B=0$, $M = 0$ and NELEM=388. Comparison with results of Refs. 6 and 15.

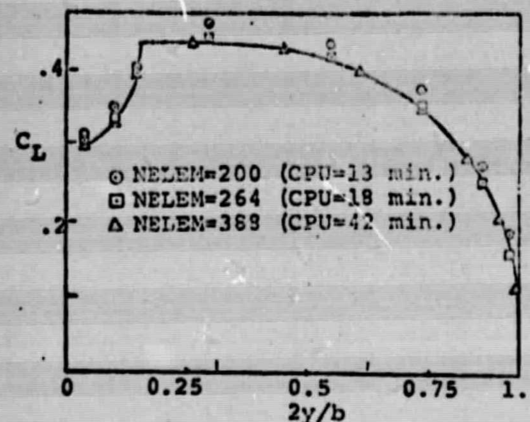

Fig. 2. Convergence study of Fig. 1 with NELEM=200, 264 and 388.

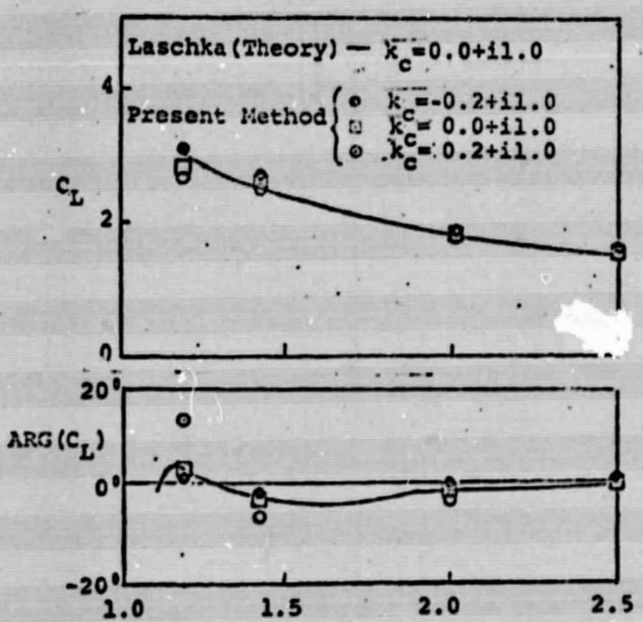

Fig. 3. Lift coefficient, C_L , for rectangular wing oscillating in pitch, with AR=2, τ=0.001, N_x=8, N_y=7. Comparison with results of Ref. 16.

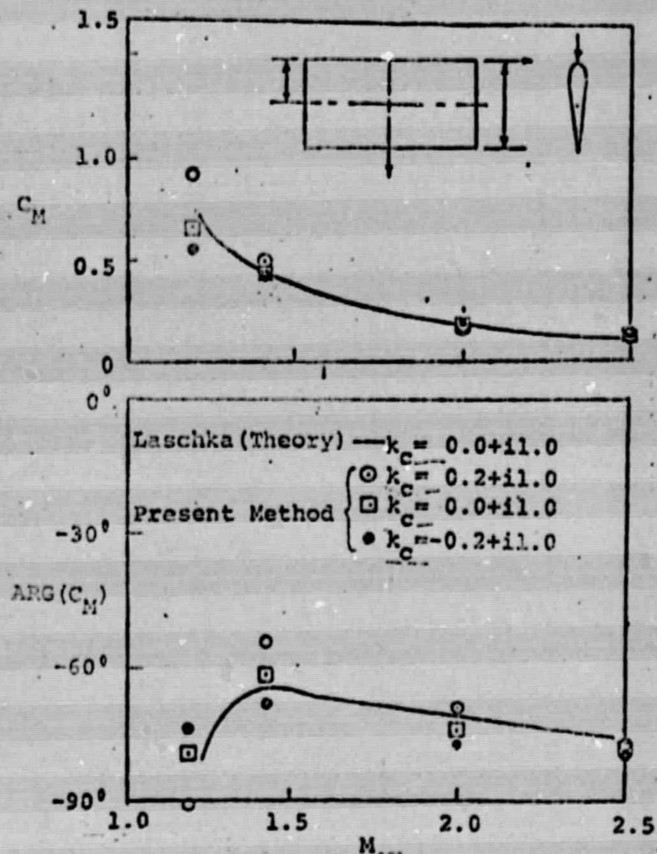

Fig. 4. Moment coefficient, C_M , versus M, for rectangular wing oscillating in pitch, for AR=2, τ=0.001, N_x=8, N_y=7. Comparison with results of Ref. 16.

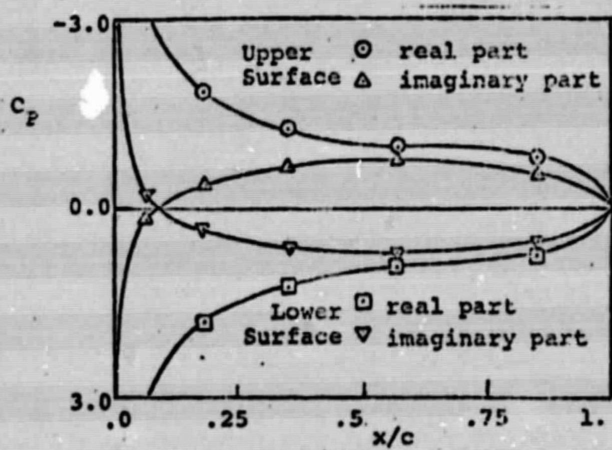

Fig. 5a. Pressure distributions at 2y/b =0.78 wing spanwise station of a wing-body-tail configuration in fully unsteady pitching mode with pitch axis at wing mid-chord. Complex frequency k_c=0.1+i1.5, span b=6, fuselage radius r^c=0.5, thickness ratio τ=.09 ,total number of elements NELEM = 388.

ORIGINAL PAGE IS
OF POOR QUALITY

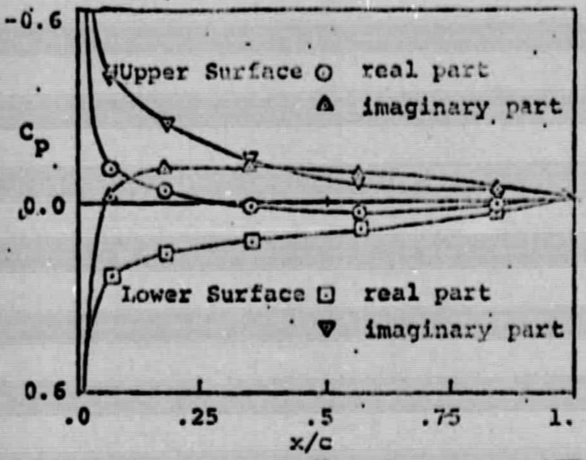

Fig. 5b. Pressure distributions at 2y/b =0.78 horizontal-tail spanwise station of the same configuration as Fig. 5a.

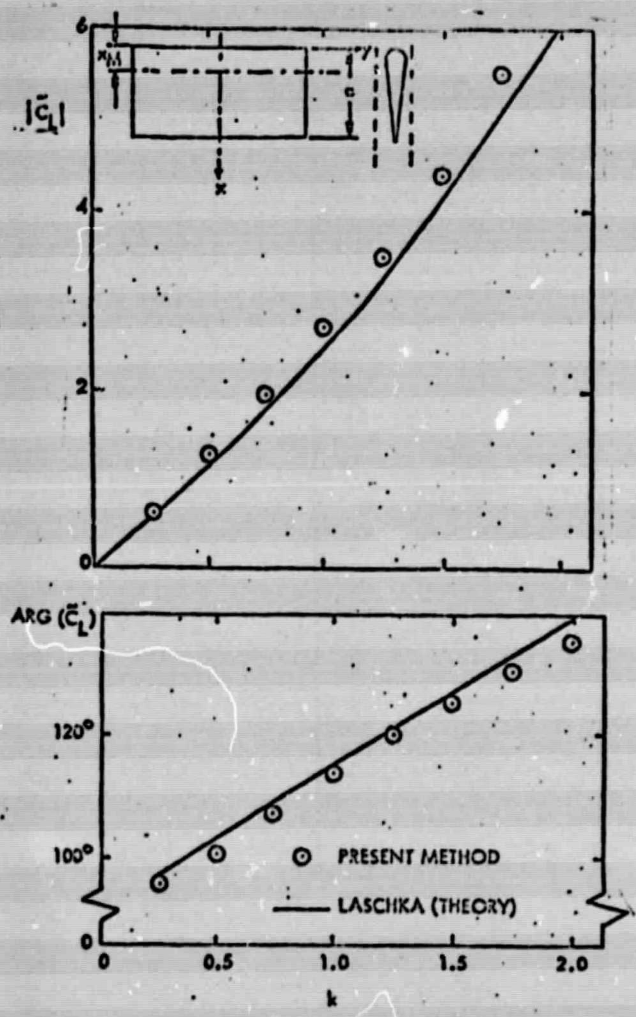

Fig. 6. Lift coefficient, $\tilde{C}_L$, versus k, for rectangular wing oscillating in plunge, with AR=2, τ=0.001, M=0, N_x=7, N_y=7, N_w=20, wake length L_w=2c. Comparison with results of Ref. 16.

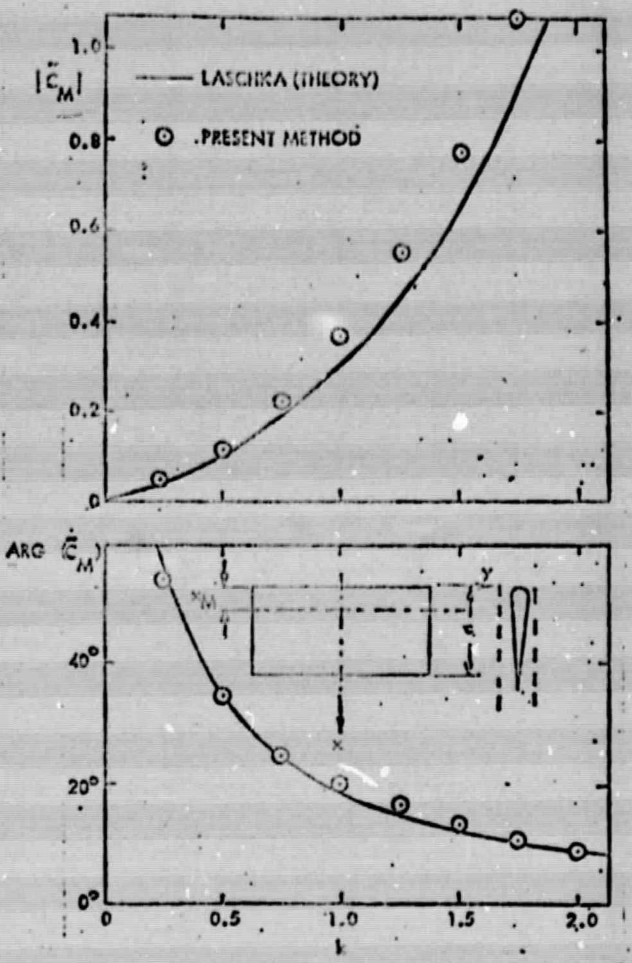

Fig. 7. Moment coefficient, $\tilde{C}_M$, versus k, for a rectangular wing oscillating in plunge, with AR=2, τ=0.001, M=0, N_x=7, N_y=7, N_w=20, wake length L_w=2c. Comparison with results of Ref. 16.

TABLE 1

Generalized Aerodynamic Force Coefficients
for AGARD Wing-Tail Interference M=0.8, Δz/L=0.6

Generalized Force in	Caused by Pressure in	i,j	k = 0.0		k = 1.5		Method
			Q'_{ij}	Q''_{ij}	Q'_{ij}	Q''_{ij}	
Wing twist	Wing twist	1,1	-0.0871	0.1726	-0.2035	0.1952	Ref. 17
			-0.0733	0.1635	-0.1644	0.1782	Ref. 18,
			-0.0600	0.0679	-0.1598	0.1335	Present
Wing bending	Wing twist	2,1	0.2611	0.3804	0.2147	0.4145	Ref. 17
			0.2776	0.3788	0.2243	0.3974	Ref. 18
			0.2272	0.2607	0.1955	0.3684	Present
Tail roll	Wing twist	3,1	-0.0619	0.0044	-0.0615	0.1246	Ref. 17
			-0.0650	0.0347	-0.0343	-0.0432	Ref. 18
			-0.0556	-0.0045	-0.0489	0.0163	Present
Tail pitch	Wing twist	4,1	-0.0206	0.0025	-0.0232	0.0108	Ref. 17
			-0.0718	0.0371	-0.0460	0.0492	Ref. 18
			-0.0154	-0.0060	-0.0181	0.0080	Present
Wing twist	Wing bending	1,2	0.0	-0.0515	-0.1360	-0.0507	Ref. 17
			0.0	-0.0440	-0.1232	-0.0387	Ref. 18
			0.0	-0.0362	-0.1163	-0.0391	Present
Wing bending	Wing bending	2,2	0.0	0.1842	-0.3478	0.2083	Ref. 17
			0.0	0.1961	-0.3303	0.2147	Ref. 18
			0.0	0.1588	-0.3317	0.2008	Present
Tail roll	Wing bending	3,2	0.0	-0.0395	-0.0431	-0.0137	Ref. 17
			0.0	-0.0420	-0.0496	0.0052	Ref. 18
			0.0	-0.0356	-0.0376	0.0122	Present
Tail pitch	Wing bending	4,2	0.0	-0.0138	-0.0192	-0.0049	Ref. 17
			0.0	-0.0459	-0.0573	0.0051	Ref. 18
			0.0	-0.0104	-0.0162	-0.0042	Present
Wing twist	Tail roll	1,3	0.0	-0.0014	-0.0008	-0.0031	Ref. 17
			0.0	0.0	-0.0008	-0.0004	Ref. 18
			0.0	-0.0004	-0.0005	-0.0018	Present
Wing bending	Tail roll	2,3	0.0	-0.0019	-0.0026	-0.0052	Ref. 17
			0.0	0.0002	-0.0015	-0.0006	Ref. 18
			0.0	-0.0002	-0.0032	-0.0036	Present
Tail Roll	Tail Roll	3,3	0.0	0.3949	-0.3156	0.4215	Ref. 17
			0.0	0.3949	-0.2974	0.4327	Ref. 18
			0.0	0.3575	-0.3638	0.3877	Present
Tail Roll	Tail Pitch	4,3	0.0	0.2519	-0.3115	0.1825	Ref. 17
			0.0	0.4255	-0.5089	0.4945	Ref. 18
			0.0	0.1270	-0.2962	0.1454	Present
Tail Pitch	Wing Twist	1,4	-0.0033	0.0005	-0.0007	-0.0016	Ref. 17
			-0.0001	0.0001	-0.0020	-0.0001	Ref. 18
			-0.0008	-0.0015	-0.0044	-0.0012	Present
Tail Pitch	Wing Bending	2,4	-0.0049	-0.0009	-0.0156	0.0012	Ref. 17
			0.0002	-0.0011	-0.0046	0.0007	Ref. 18
			-0.0014	-0.0022	-0.0120	0.0002	Present
Tail Pitch	Tail Roll	3,4	0.6345	0.6975	0.5328	0.7713	Ref. 17
			0.6775	0.9986	0.3278	1.0701	Ref. 18
			9.6400	0.7223	0.3916	0.7766	Present
Tail Pitch	Tail Pitch	4,4	0.1866	0.5611	-0.0452	0.6442	Ref. 17
			0.7205	1.4769	-0.0264	1.6094	Ref. 18
			0.1590	0.4381	-0.1496	0.5354	Present
Wing Twist & Tail Roll	Wing Twist & Tail Roll	1+3, 1+3	-0.1470	0.5492	-0.5713	0.6274	Ref. 19
			-0.1156	0.4254	-0.5661	0.5346	Present
Wing Twist & Tail Roll	Wing Bending & Tail Pitch	2+4, 1+3	0.2404	0.5308	-0.1262	0.5984	Ref. 19
			0.2117	0.4990	-0.1300	0.5226	Present
Wing Bending & Tail Pitch	Wing Twist & Tail Roll	1+3, 2+4	0.6402	0.6181	0.3558	0.7180	Ref. 19
			0.6351	0.6475	0.2332	0.7243	Present
Wing Bending & Tail Pitch	Wing Bending & Tail Pitch	2+4, 2+4	0.1619	0.7565	-0.4568	0.8729	Ref. 19
			0.1694	0.6266	-0.5094	0.7317	Present

ORIGINAL PAGE IS
OF POOR QUALITY

TABLE 2

Generalized Aerodynamic Force Coefficients
for AGARD Wing-Tail Interference M=3.0, z/L=0.6

Generalized Force in	Caused by Pressure in	i,j	$k = 1.5$ Q'_{ij}	Q''_{ij}	Method
Wing twist	Wing twist	1,1	0.0913	0.1462	Ref. 20
			0.1059	0.1446	Ref. 21
			0.1172	0.1318	Present
Wing bending	Wing twist	2,1	0.3801	0.0890	Ref. 20
			0.2710	0.1207	Ref. 21
			0.3387	0.0824	Present
Tail roll	Wing twist	3,1	0.1253	0.0554	Ref. 20
			-0.0137	0.1024	Ref. 21
			-0.1566	-0.0315	Present
Tail pitch	Wing twist	4,1	0.0856	0.0541	Ref. 20
			-0.0068	0.0817	Ref. 21
			-0.0376	-0.0406	Present
Wing twist	Wing bending	1,2	-0.0746	0.0301	Ref. 20
			-0.0294	0.0801	Ref. 21
			-0.0433	0.0596	Present
Wing bending	Wing bending	2,2	-0.0729	0.2447	Ref. 20
			0.0167	0.2464	Ref. 21
			-0.0248	0.2218	Present
Tail roll	Wing bending	3,2	-0.0491	0.0615	Ref. 20
			-0.0715	-0.0012	Ref. 21
			0.0358	-0.0908	Present
Tail pitch	Wing bending	4,2	-0.0406	0.0485	Ref. 20
			-0.0602	0.0104	Ref. 21
			0.0338	-0.0606	Present
Tail roll	Tail roll	3,3	0.0163	0.2622	Ref. 20
			0.0700	0.3170	Ref. 21
			0.0409	0.2898	Present
Tail pitch	Tail roll	4,3	0.0072	0.1864	Ref. 20
			0.0365	0.2208	Ref. 21
			0.0263	0.2240	Present
Tail roll	Tail pitch	3,4	0.4517	0.1632	Ref. 20
			0.4410	0.2168	Ref. 21
			0.5000	0.1874	Present
Tail pitch	Tail pitch	4,4	0.2965	0.2588	Ref. 20
			0.3162	0.3010	Ref. 21
			0.3724	0.2354	Present

TABLE 3a

Generalized Aerodynamic Force Coefficients
for AGARD Wing-Tail Interference M=0.8, $\Delta z/L=0.6$

Generalized Force in	Caused by Pressure in	i,j	$k_c = -0.2 + i1.5$		$k_c = 0.0 + i1.5$		$k_c = 0.2 + i1.5$	
			Q'_{ij}	Q''_{ij}	Q'_{ij}	Q''_{ij}	Q_{ij}	$-Q''_{ij}$
Wing twist	Wing bending	1,2	-0.1208	-0.0452	-0.1467	-0.0242	-0.1408	-0.0033
Wing bending	Wing bending	2,2	-0.2984	0.0934	-0.3783	0.1956	-0.3903	0.2536
Tail roll	Wing bending	3,2	-0.0641	-0.0595	-0.0311	-0.0124	-0.0251	-0.0120
Tail pitch	Wing bending	4,2	-0.0158	-0.0393	-0.0148	-0.0042	-0.0122	-0.0028

TABLE 3b

Generalized Aerodynamic Force Coefficients
for AGARD Wing-Tail Interference M=3.0, $\Delta z/L=0.6$

Generalized Force in	Caused by Pressure in	i,j	$k_c = -0.15+i1.5$		$k_c = 0.0+i1.5$		$k_c = 0.15+i1.5$	
			Q'_{ij}	Q''_{ij}	Q'_{ij}	Q''_{ij}	Q'_{ij}	Q''_{ij}
Wing twist & Tail roll	Wing twist & Tail roll	1+3, 1+3	-0.0298	0.4090	0.0130	0.4004	0.0464	0.3933
Wing bending & Tail pitch	Wing twist & Tail roll	2+4, 1+3	0.2373	0.2855	0.2654	0.2860	0.2872	0.2858